

# From Generator to Embedder: Harnessing Innate Abilities of Multimodal LLMs via Building Zero-Shot Discriminative Embedding Model

Yeong-Joon Ju and Seong-Whan Lee, *Fellow, IEEE*

**Abstract**—Multimodal Large Language Models (MLLMs) have emerged as a promising solution for universal embedding tasks, yet adapting their generative nature for discriminative representation learning remains a significant challenge. The dominant paradigm of large-scale contrastive pre-training suffers from critical inefficiencies, including prohibitive computational costs and a failure to leverage the intrinsic, instruction-following capabilities of MLLMs. To overcome these limitations, we propose an efficient framework for universal multimodal embeddings, which bridges this gap by centering on two synergistic components. First, our hierarchical embedding prompt template employs a two-level instruction architecture that forces the model to produce discriminative representations. Building on this strong foundation, our second component, self-aware hard negative sampling, redefines the fine-tuning process by leveraging the model’s own understanding to efficiently mine challenging negatives while actively filtering out potential false negatives. Our comprehensive experiments show that our hierarchical prompt achieves zero-shot performance competitive with contrastively trained baselines and enhances the fine-tuning process by lifting a simple in-batch negative baseline by 4.8 points on the MMEB benchmark. We further boost the performance via our self-aware hard negative sampling, achieving the state-of-the-art performance without the contrastive pre-training. Our work presents an effective and efficient pathway to adapt MLLMs for universal embedding tasks, significantly reducing training time.

**Index Terms**—Multimodal Large Language Models, Multimodal Embeddings, Prompt Engineering, Contrastive Learning, Hard Negative Mining.

## I. INTRODUCTION

Embeddings [1], [2] are fixed-dimensional representations of inputs, encoded as semantic information within a continuous vector space, underpinning various downstream tasks such as clustering [3], [4], retrieval [5]–[8], and classification [9]. Following the success of instruction-based multi-task training methods [10], [11], the focus of research has shifted toward achieving universal embeddings [12]–[14], where a single model provides robust representations across diverse tasks and domains. The rapid growth of multimedia applications has further driven the need for universal multimodal embeddings [15]–[18] capable of supporting both uni-modal and cross-modal retrieval.

Y.-J. Ju and S.-W. Lee are with in the Department of Artificial Intelligence at Korea University, Seoul, Republic of Korea. This work was supported by the Institute of Information & Communications Technology Planning & Evaluation (IITP) grant, funded by the Korea government (MSIT) (No. RS-2019-II190079 (Artificial Intelligence Graduate School Program (Korea University)), No. IITP-2025-RS-2024-00436857 (Information Technology Research Center (ITRC)). Corresponding author: Seong-Whan Lee. E-mail: yj\_ju@korea.ac.kr, sw.lee@korea.ac.kr

For multimodal embeddings, the prevailing approaches [15], [19], [20] have primarily relied on the pre-trained CLIP [21] or BLIP [22], which initially encode image and text separately. Although they have achieved remarkable performance, these architectures struggle with interleaved or text-heavy visual-language inputs due to their lack of in-depth image-text fusion [23]–[25], limiting their applicability for general-purpose tasks. To address these limitations, multimodal large language models (MLLMs) [26] have emerged as a promising solution for embedding tasks. Built upon decoder-only transformers, MLLMs inherit powerful emergent abilities [27] from their large language model (LLM) counterparts, such as instruction-following and in-context learning. Crucially, their pre-training on interleaved visual and textual data allows them to capture complex cross-modal dependencies, offering a promising architectural alternative to address the weaknesses of dual-encoders.

Despite this potential, adapting MLLMs for embedding tasks remains a significant challenge. Their inherent training objective of next-token prediction is optimized for generating coherent sequences, not for producing a single and compact embedding that represents the entire input. To bridge this functional gap between generation and embedding, the dominant paradigm [17], [28]–[32] has relied on large-scale contrastive pre-training that extensively fine-tunes MLLMs on massive paired datasets to impart discriminative properties. However, this paradigm suffers from critical inefficiencies. First, large-scale contrastive pre-training incurs prohibitive computational costs by demanding massive paired datasets and extensive fine-tuning of large models. Second, and more fundamentally, the approach underutilizes the intrinsic emergent abilities of MLLMs by treating them as conventional encoders. Such reliance on data scale over innate model capability escalates resource dependency. To prevent catastrophic forgetting of the model, existing methods [30], [31] often introduce further complexities. For instance, they require joint training with a generation loss, complicating an already burdensome process.

We identify the overlooked potential of prompts as a crucial starting point. While recent studies, such as E5-V [17] and VladVA [31], have shed some light on the importance of prompts, they have primarily focused on utilizing them from the perspective of text transformation for compressing information into an embedding. This overlooks a more fundamental question that our work focuses on: how can we systematically structure prompts to elicit powerful discriminative embeddings in a zero-shot manner?

In this paper, we propose a framework that mitigates these inefficiencies by leveraging the MLLM’s inherent capabilities to bridge the gap to the multimodal embedding task. Our method is centered around two synergistic components. The first component of our framework is the hierarchical embedding prompt template, which employs a two-level instruction hierarchy. This template leverages a system-level prompt that defines a consistent objective for all inputs and reinforces the objective in a user-level prompt. Building upon this zero-shot foundation, our second component is self-aware hard negative sampling (SaHa), an efficient fine-tuning strategy that redefines hard negative mining.

Recent approaches [28], [32], [33] often rely on external teacher models or use a similarity-based thresholding, which can be computationally intensive and prone to selecting false negatives. In contrast, our sampling method leverages the model’s own understanding to mine more effective negatives. We also enhance the efficiency of hard negative training by minimizing the reuse of negative candidates. Our core intuition is that similar queries have similar targets. For a given anchor, we first retrieve a set of candidates semantically similar to the anchor query. Instead of using these candidates directly, we identify the adjacent queries linked to each candidate. To filter out potential false negatives, we then select candidates belonging to the most dissimilar queries from this group as hard negatives for the anchor query. This process clusters samples that are challenging yet distinct without depending on any external models.

Our comprehensive experiments reveal that our hierarchical prompt plays a crucial dual role, by first establishing a competitive zero-shot baseline and then directly enhancing the subsequent fine-tuning process. Building on this strong foundation from the prompt, our SaHa effectively mitigates the issue of false negative contamination, thereby achieving state-of-the-art performance. This approach is also highly efficient, drastically reducing the prohibitive training costs of conventional methods. Our work presents an effective and efficient pathway to bridge the emergent abilities of MLLMs to universal multimodal embedding tasks. Our main contributions are summarized as follows:

- We propose a hierarchical embedding prompt, a systematic template that guides MLLMs toward high-quality, discriminative embeddings. This prompt achieves competitive zero-shot performance on its own and provides a strong foundation for efficient fine-tuning.
- We introduce Self-aware Hard negative sampling (SaHa), a sampling strategy for efficient fine-tuning, which leverages the model’s own understanding to mine hard negatives. SaHa filters out potential false negatives without relying on external teacher models, significantly reducing the computational overhead of the training process.
- We demonstrate the effectiveness and synergy of our approach through comprehensive experiments. Our hierarchical prompt significantly enhances fine-tuning, improving a standard in-batch negative baseline by 4.8 points on the MMEB benchmark. Our framework, combining the prompt and SaHa, achieves state-of-the-art performance, even when compared against methods that require large-

scale contrastive pre-training.

## II. RELATED WORK

Traditional information retrieval methods, such as TF-IDF and BM25 [34], relied on keyword matching, often failing to capture the deeper semantics of inputs. The advent of dense retrieval methods [5], [12], [35]–[37] marked a paradigm shift, leveraging pre-trained language models, such as BERT [2] and T5 [38], to encode rich semantic information into embedding vectors.

### A. Multimodal Retrieval

The need to process inputs that combine vision and language has driven the development of multimodal retrieval. Early approaches focused on enriching the input by converting images into richer textual representations, such as captions [39]–[41] or object tags [42]–[44]. To eliminate the dependency on such intermediate modules, subsequent research [16], [24], [25] shifted towards end-to-end retrieval systems that employ in-depth fusion between modalities. Following the success of multi-task training in text embeddings [10], [11], recent studies [16], [20] leveraged instruction-following tuning to handle heterogeneous queries and candidates in diverse modalities, pushing the boundaries towards universal multimodal embeddings. However, their reliance on architectures with separate initial encoders still posed a challenge for achieving a universal multimodal embedding space.

### B. Universal Embeddings

To overcome the task-specific nature of earlier models, research on universal embeddings aims to create a single model that provides robust representations across a diverse range of tasks and domains. The success of LLMs as backbones for text-only embeddings has been demonstrated by numerous studies [45]–[48], showing that large-scale models possess strong capabilities for producing powerful representations.

While previous approaches [16], [20] for universal multimodal embeddings enhanced dual-encoders with more sophisticated fusion, they still operated on separately encoded modalities. This fundamental architectural limitation motivated the shift toward MLLMs. By pre-training on interleaved visual and textual data, MLLMs can capture complex cross-modal dependencies natively, emerging as a promising solution to the weaknesses of dual-encoders. The dominant paradigm for adapting their generative nature for discriminative embedding tasks is large-scale contrastive fine-tuning. Within this paradigm, various strategies have been proposed. VLM2Vec [18] and MM-Embed [49] fine-tune MLLMs on extensive, diverse multimodal task datasets to create a universal embedding space. Others focus on the critical role of training data. MegaPairs [50] and GME [29] introduce large-scale data synthesis pipelines to generate high-quality image-text pairs with open-ended instructions, thereby enhancing model performance on universal retrieval benchmarks.

A parallel line of research investigates how to preserve the generative strengths of MLLMs during this discriminative fine-tuning. VladVA [31] and CAFe [30] propose joint training

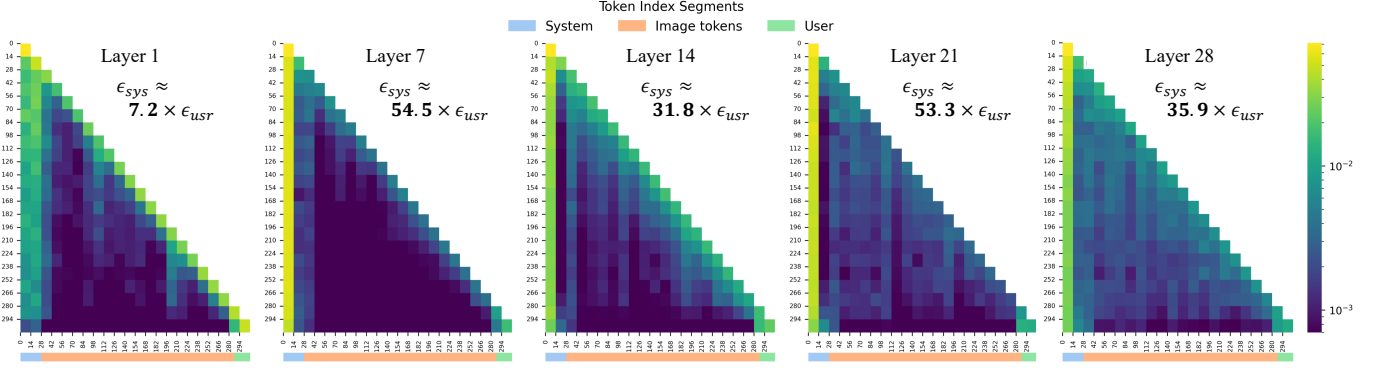


Fig. 1: **Analysis of attention weights on token types.** Across various layers of the MLLM, system prompt tokens (blue) consistently receive significantly higher attention weights compared to user prompt tokens (green). The value  $\epsilon_{sys}$  denotes the average attention weight for system tokens, while  $\epsilon_{usr}$  is for user tokens.

frameworks that combine contrastive loss with a next-token prediction loss. This allows the model to learn discriminative representations without suffering from catastrophic forgetting of its generative capabilities. UNITE [32] has pushed this further by analyzing modality-specific data properties and proposing a modality-aware contrastive learning objective to mitigate interference between different modalities during training. Despite these advances, the prevailing methods still rely on computationally expensive, large-scale contrastive pre-training and complex training objectives. This highlights a clear gap for our efficient framework that unlock the powerful, inherent discriminative capabilities of MLLMs.

### III. METHODS

Our framework adapts a pre-trained Multimodal Large Language Model (MLLM) for universal multimodal embedding tasks via two components: a zero-shot prompting strategy designed to unlock the model’s innate capabilities, and a highly efficient fine-tuning process to further maximize performance. We describe each component in detail below.

#### A. Preliminaries: Multimodal Embedding with MLLMs

Our framework is built upon a pre-trained MLLM. A typical MLLM synergistically integrates three core components: (1) a vision encoder (e.g., ViT [51]) that processes visual information, (2) a projection layer that aligns image features into the linguistic space of LLM, and (3) an LLM backbone (e.g., LLaMA [52]) that processes the unified sequence of visual and textual tokens. This architecture enables a deep, contextualized understanding of interleaved data.

The primary goal of a universal multimodal embedding model  $f(\cdot)$  is to map heterogeneous multimodal inputs, such as text, images, or interleaved combinations, into a shared, fixed-dimensional vector space. For a given query  $q$  and a collection of candidates, the objective is to ensure high similarity  $S(f(q), f(c^+))$  between the query  $q$  and the most relevant (positive) candidate  $c^+$  while retaining relatively low similarity for irrelevant (negative) candidates  $c^-$ , where  $S$  is typically the cosine similarity. Following existing approaches [17], [18], [47] for decoder-only transformers, the final embedding

is obtained by selecting the hidden state of the last input token from the model’s output hidden states (i.e., last token pooling). The extracted final embedding then undergoes L2-normalization.

#### B. Hierarchical Embedding Prompt for Zero-Shot Power

To bridge the MLLM’s generative pre-training with the discriminative needs of embedding tasks, we introduce a prompting strategy, motivated by an empirical analysis of how MLLMs differentially process instructions.

1) *The Influential Role of System Prompts:* Recent works [53], [54] have analyzed attention mechanisms for generative efficiency on MLLMs, finding that visual tokens often receive less attention while system prompts act as highly-attended anchor tokens guiding the entire generation process. Unlike their work focused on generative efficiency, we investigate how this privileged role of the system prompt can be repurposed to create a discriminative representation space. We hypothesized that this anchor function could serve as a global controller, enforcing a consistent structure across all inputs (queries and candidates) to align them within a shared embedding space.

To quantify our hypothesis, we adapt the attention efficiency from FastV [53], which measures the average attention a token type receives per token. Formally, for a given token type (e.g., system, user), its attention efficiency  $\epsilon$  is:

$$\epsilon_{\text{type}} = \frac{\sum_{i=1}^{N_{\text{out}}} \alpha_{\text{type}}^i}{|T_{\text{type}}|}, \quad (1)$$

where  $\alpha_{\text{type}}^i$  is the summed attention from the  $i$ -th output token to all tokens of that type,  $N_{\text{out}}$  is the number of output tokens, and  $|T_{\text{type}}|$  is the token count for that type. We measured the causal attention weights for all input tokens. As shown in Fig. 1,  $\epsilon_{sys}$  is substantially greater than  $\epsilon_{usr}$ , suggesting the system prompt acts as a global controller that fundamentally shapes the entire representation space.

2) *Hierarchical Prompting Strategy:* To leverage this intrinsic functional hierarchy, we propose the hierarchical embedding prompt template. As illustrated in Fig. 2, our strategy decouples instructions into two levels:

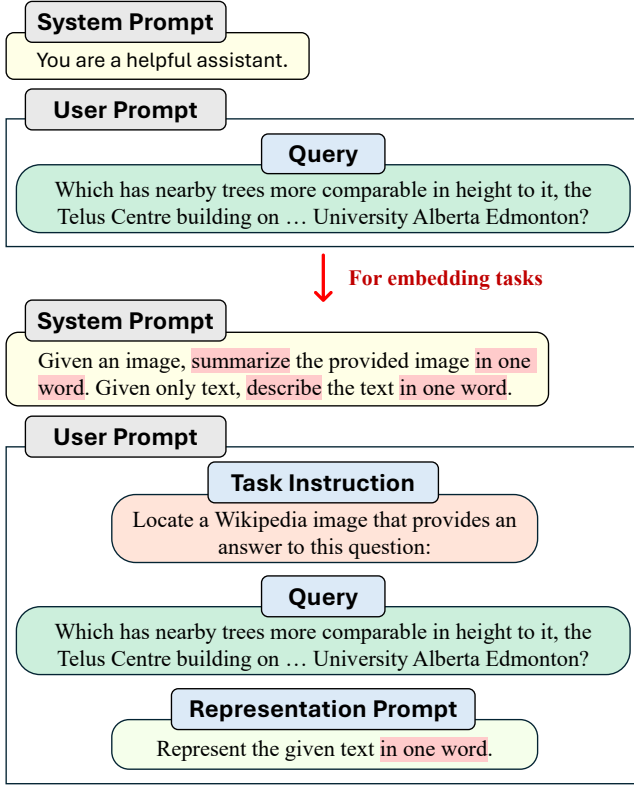


Fig. 2: An example of our hierarchical embedding prompt.

**Level 1: System Prompt.** A universally applied instruction for all inputs (both queries and candidates). The purpose of the global prompt is to enforce semantic compression that aligns all inputs into a structurally coherent embedding space. By leveraging the system prompt’s role as a global controller, this approach creates a stable foundation for embedding tasks.

**Level 2: Representation Prompt.** An instruction applied only to the query to reinforce the embedding objective. In the user prompt, a task instruction specifies the embedding task’s intent and format (e.g., Identify the object depicted in the image). However, the complexity of the task instruction or the query’s own content could inadvertently steer the model away from the global objective defined by the system prompt (e.g., causing it to generate an answer instead of an embedding). To counteract this and explicitly reinforce the global objective, we append a representation prompt at the end of the query input. This final instruction acts as a safeguard, ensuring the model’s output remains focused on the embedding compression task and does not deviate.

This hierarchical design allows the model to maintain a stable global embedding structure while precisely adapting the query’s focus, enabling powerful zero-shot discriminative performance. The specific prompt format used to implement this strategy is as follows:

For a query input:

**System:** Given an image, summarize the provided image in one word. Given only text, describe the text in one word.

**User:** [ Task Instruction ]  
[ Query ] [ Representation Prompt ]  
**Assistant:**

For a candidate document input:

**System:** Given an image, summarize the provided image in one word. Given only text, describe the text in one word.  
**User:** [ Candidate ]  
**Assistant:**

### C. Self-aware Hard Negative Sampling

Traditional hard negative sampling (HNS) methods aim to improve model performance by mining for negative samples that are semantically similar to a given anchor query  $q$ . However, this approach presents two drawbacks. First, HNS suffers from false negative contamination, as it inadvertently samples unlabeled positives as negatives ( $c^-$ ). This process fundamentally corrupts the contrastive learning objective by penalizing the model for recognizing valid semantic similarities. Second, HNS creates a severe computational imbalance by requiring  $N \times k$  candidate inferences for a batch of  $N$  queries with  $k$  negatives each. This multiplicative overhead presents a core computational bottleneck, motivating the development of more efficient sampling strategies (e.g., in-batch negative sampling). To address the contamination issue, the previous method [28] has attempted to apply a similarity-based threshold, excluding any negatives with a score higher than a predefined margin (e.g., a  $\beta$ -margin). However, this method introduces its own challenges. The optimal similarity threshold varies significantly across different tasks and datasets, making a universal value difficult to set. This, in turn, renders the model’s performance highly sensitive to this hyperparameter. They are also limited in handling the modality of training data due to the use of an LLM-based teacher model.

To overcome these limitations, we present Self-aware Hard Negative Sampling (SaHa) to construct clusters of mutually challenging samples while preventing the false negative contamination. SaHa leverages the target model to be trained, enhanced through our hierarchical embedding prompt, to guide the sampling process based on its own representational space. Our core intuition is that similar queries have similar targets. Under this intuition, we build a “cluster” of  $N$  (query, positive candidate) pairs to enable the model to learn fine-grained discriminative representations. Our process unfolds as follows:

Let  $k$  denote the desired number of hard negatives. To ensure all samples in the cluster are relevant, we first retrieve a larger set of semantically similar candidates  $D_{cand}$  for an anchor query  $q$ , such that  $|D_{cand}| > k$ . This step establishes a pool of challenging candidates. Subsequently, we shift to the query perspective by identifying the “owner” queries  $Q_{adj}$ , which are queries from the training set in which a retrieved candidate serves as the positive target. When a candidate is linked to multiple queries in the training set (as is often the case in classification tasks), we assign the query most similar to the anchor query as its owner. This strategy reinforces

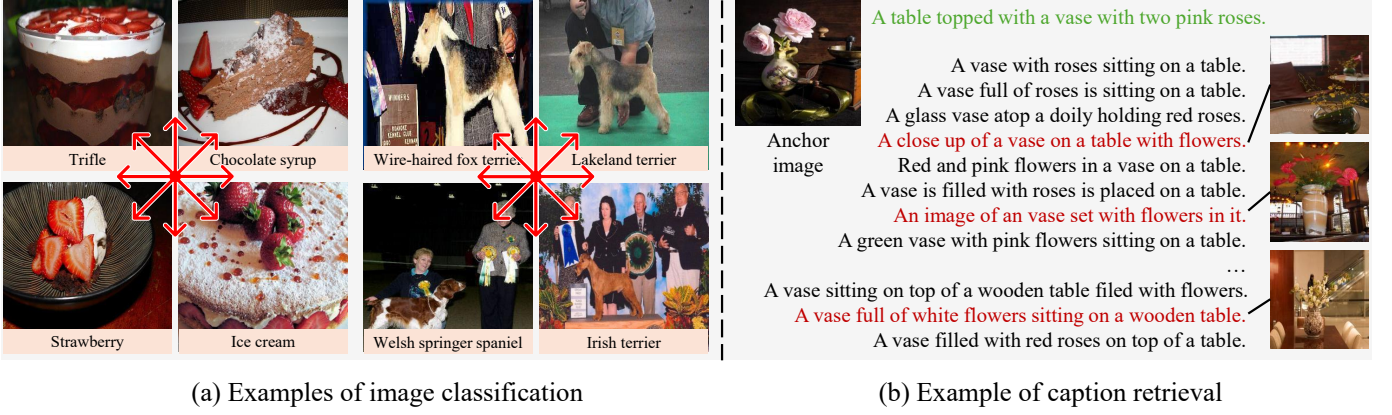


Fig. 3: **Qualitative examples illustrating SaHa’s sampling mechanism.** The strategy composes batches with negatives that are semantically challenging yet reliable. (a) For a given anchor image, SaHa selects negatives from the same thematic cluster (e.g., desserts that both contain strawberries, or dogs with similar side profiles alongside people) but with different class identities. (b) For caption retrieval, SaHa selects a caption (in red) that is thematically related but represents a different semantic meaning, effectively avoiding potential false negatives (a positive candidate in green).

semantic alignment with the anchor while exploiting the candidate’s ambiguity to construct stronger hard negatives. Finally, to complete the cluster, we select the  $k$  candidate–owner query pairs whose owner queries are least similar to the anchor query  $q$ . This helps avoid potential false negatives, since semantically similar queries are more likely to share the same target and thus may not serve as reliable negatives. The SaHa procedure is performed as a one-time, offline pre-processing step before fine-tuning. We detail this process in Algorithm 1. In phase 1, we enforce non-overlapping cluster assignments to minimize redundancy. In phase 2, we allow limited duplication for a small number of samples unassigned in phase 1, ensuring that all samples are eventually included in a cluster.

Fig. 3 provides qualitative examples of this batch construction process. Fig. 3(a) demonstrates how SaHa populates the batch with challenging negatives by selecting candidates with common features, forcing the model to learn fine-grained distinctions. The caption retrieval example in Fig. 3(b) demonstrates how the process effectively excludes potential false negatives. These examples visually confirm that SaHa builds batches with negatives that are both challenging and reliable.

**Training Objective.** For each anchor query  $q_i$ , our SaHa strategy constructs a dedicated training cluster. This cluster contains the anchor’s positive pair  $(q_i, c_i^+)$  along with the  $k$  hard negative pairs  $\{(q_j, c_j^+)\}_{j=1}^k$  selected by our sampling process. Thus, each cluster is composed of  $k + 1$  (query, positive candidate) pairs. We then employ an in-batch negative sampling strategy within this tailored cluster. For the anchor query  $q_i$ , its corresponding positive is  $c_i^+$ , and the positive candidates from the other  $k$  pairs in the cluster,  $\{c_j^+\}_{j=1}^k$ , serve as its hard negatives. We fine-tune the model using the Noise Contrastive Estimation (InfoNCE) loss [55] as follows:

$$\mathcal{L}_i = -\log \frac{e^{S(f(q_i), f(c_i^+))/\tau}}{e^{S(f(q_i), f(c_i^+))/\tau} + \sum_{j=1, j \neq i}^B e^{S(f(q_i), f(c_j^+))/\tau}}, \quad (2)$$

where  $\tau$  is a temperature hyper-parameter. Note that we process  $B$  such clusters in parallel, making our effective training batch size  $B \times (k + 1)$ .

#### IV. EXPERIMENTS

In this section, we present a comprehensive set of experiments to validate the effectiveness and efficiency of our proposed framework. First, we demonstrate that our hierarchical embedding prompt elicits powerful zero-shot embedding capabilities from MLLMs without any task-specific training. Second, we conduct in-depth ablation studies to analyze the contribution of each component of our prompt. Third, we show that fine-tuning with our SaHa strategy outperforms our MLLM baselines with significantly greater efficiency than baselines for hard negative sampling. Finally, we analyze the effectiveness and stability of the SaHa strategy.

##### A. Experimental Setup

Our experiments are built upon the Qwen2-VL [56] model, which serves as our base architecture. Unless otherwise specified, our analyses and ablation studies are conducted on the 2.2B model (Qwen2-VL-2B) for efficiency. However, our framework is model-agnostic and not limited to any specific MLLM architecture.

**Implementation Details.** For fine-tuning, we used the AdamW optimizer [57] with a learning rate of  $5 \times 10^{-5}$  and a linear learning rate schedule with a 100-step warm-up phase. The temperature  $\tau$  and the maximum sequence length were set to 0.02 and 1024 tokens, respectively. The model was trained for 1.5 epochs using a LoRA adapter with a rank of 8. While we resized the input images to a fixed  $448 \times 448$  resolution during training, we allowed for dynamic resolutions at inference. Following the previous work [18], we employed GradCache [58], a gradient caching method, to increase the effective batch size beyond our hardware limitations, with a sub-batch size of 16. For the large model (Qwen2-VL-7B),



**Algorithm 1: Self-aware Hard Negative Sampling**

**Input:**  $Q_{full}$ : The entire set of queries  
 $C$ : The entire set of candidate documents  
 $D2Q$ : A dictionary mapping a document to its list of owner queries  
 $k$ : The number of hard negatives to sample  
 $m$ : Pool multiplier to set the initial candidate pool size.  
**Output:**  $H$ : The final training set.

```

1 Function CoupleSamples( $Q_{sub}, U_{global}$ )
2    $H_{local} \leftarrow \emptyset$ 
3    $U_{local} \leftarrow \emptyset$ 
4   if  $|U_{global}| > 0$  then allow_redundancy  $\leftarrow$  True
5   else allow_redundancy  $\leftarrow$  False
6   for each query  $q \in Q_{sub}$  do
7     if  $q \notin U_{global}$  then
8        $D_{cand} \leftarrow \text{Retrieve}(q, I_C)[m \times k]$ 
9        $Q_{adj} \leftarrow \emptyset$ 
10      for each document  $d \in D_{cand}$  do
11        if  $d \in D2Q$  then
12          if  $|D2Q[d]| > 1$  then
13             $q_{owner} \leftarrow \text{Retrieve}(q, D2Q[d])[0]$ 
14          else
15             $q_{owner} \leftarrow D2Q[d][0]$ 
16           $Q_{adj} \leftarrow Q_{adj} \cup \{q_{owner}\}$ 
17      if allow_redundancy then
18         $U_{de-dup} \leftarrow U_{local}$ 
19      else  $U_{de-dup} \leftarrow U_{global}$ 
20       $Q_{adj} \leftarrow Q_{adj} \setminus U_{de-dup}$ 
21       $Q_{sorted} \leftarrow \text{SortByAscendingSimilarity}(Q_{adj}, q)$ 
22       $Q_{neg} \leftarrow$  first  $k$  queries from  $Q_{sorted}$ 
23       $H_{local} \leftarrow H_{local} \cup \{(q, c^+, \text{GetRows}(Q_{neg}))\}$ 
24       $U_{global} \leftarrow U_{global} \cup \{q\} \cup Q_{neg}$ 
25      if allow_redundancy then
26         $U_{local} \leftarrow U_{local} \cup Q_{neg}$ 
27  return  $H_{local}$ 

// Main Process
26  $H \leftarrow \emptyset, U \leftarrow \emptyset$ 
27  $I_C \leftarrow \text{BuildGlobalIndex}(C)$ 
29 Phase 1: Primary Mining
30  $H \leftarrow \text{CoupleSamples}(Q_{full}, U)$ 
32 Phase 2: Leftover Processing
33  $Q_{leftover} \leftarrow Q_{full} \setminus U$ 
34  $H_{leftover} \leftarrow \text{CoupleSamples}(Q_{leftover}, U)$ 
35  $H \leftarrow H \cup H_{leftover}$ 
36 return  $H$ 

```

**TABLE I: The statistics of the MMEB dataset.**

Meta-Task	Dataset	#Training	#Eval
Classification (10 Tasks)	ImageNet-1K	100K	1000
	N24News	49K	1000
	HatefulMemes	8K	1000
	VOC2007	8K	1000
	SUN397	20K	1000
	Place365	-	1000
	ImageNet-A	-	1000
	ImageNet-R	-	1000
	ObjectNet	-	1000
	Country-211	-	1000
VQA (10 Tasks)	OK-VQA	9K	1000
	A-OKVQA	17K	1000
	DocVQA	40K	1000
	InfographicVQA	24K	1000
	ChartQA	28K	1000
	Visual7W	70K	1000
	ScienceQA	-	1000
	VizWiz	-	1000
	GQA	-	1000
	TextVQA	-	1000
Retrieval (12 Tasks)	VisDial	123K	1000
	CIRR	26K	1000
	VisualNews_t2i	100K	1000
	VisualNews_i2t	100K	1000
	MSCOCO_t2i	100K	1000
	MSCOCO_i2t	113K	1000
	NIGHTS	16K	1000
	WebQA	17K	1000
	OVEN	-	1000
	FashionIQ	-	1000
	EDIS	-	1000
	Wiki-SS-NQ	-	1000
Visual Grounding (4 Tasks)	MSCOCO	100K	1000
	Visual7W-Pointing	-	1000
	RefCOCO	-	1000
	RefCOCO-Matching	-	1000

the sub-batch size was set to 4. All training experiments were conducted on  $8 \times$  RTX A6000 GPUs.

**Datasets.** We evaluate our model on the Massive Multimodal Embedding Benchmark (MMEB) [18], which comprises 36 datasets across four meta-tasks: Classification (Cla.), Visual Question Answering (VQA), Retrieval (Ret.), and Visual Grounding (Gro.). All tasks are evaluated in an embedding-based retrieval manner. For instance, a VQA task is treated as a retrieval problem where the model should find the embedding of the correct textual answer from a set of candidates that is most similar to the embedding of the image-question pair. For fine-tuning, we use the combined training sets from 20 in-domain (IND) datasets ( $\sim 829K$  pairs). The remaining 16 out-of-domain (OOD) datasets are used exclusively for zero-shot evaluation. The dataset statistics are provided in Table I. We report Precision@1 for the MMEB benchmark.

In addition, to conduct analyses of image-text compositionality, we use the SugarCrepe [59] and SugarCrepe++ [60] benchmarks. These benchmarks are specifically designed to test a model’s ability to understand subtle semantic changes in image captions, such as swapping objects or attributes. In the case of SugarCrepe++, we evaluate under two settings: the multi-modal Image-to-Text (ITT) setting and the uni-modal Text-only (TOT) setting, which isolates the text encoder’s

TABLE II: **Zero-shot Performance on the MMEB.** Our training-free method, which solely relies on our hierarchical prompt, is compared against various contrastively trained vision-language models (VLMs) and MLLMs.

Method	#Params	Cla.	VQA	Ret.	Gro.	Avg.
Contrastive VLMs						
CLIP [21]	0.4B	42.8	9.1	53.0	51.8	37.8
OpenCLIP [61]	0.4B	47.8	10.9	52.3	53.3	39.7
SigLIP [62]	0.9B	40.3	8.4	31.6	59.5	34.8
MagicLens [63]	0.4B	38.8	8.3	35.4	26.0	27.1
Contrastive MLLMs						
E5-V [17] (LLaVA-NeXT [64])	8.4B	21.8	4.9	11.5	19.0	13.3
UniME [28] (Phi3.5-V [65])	4.2B	42.5	18.3	40.5	59.9	40.3
MMRet [50] (LLaVA-1.6 [66])	7.8B	47.2	18.4	56.5	62.6	44.0
Training-Free MLLMs						
Qwen2-VL-2B [56]	2.2B	21.4	8.9	9.5	21.2	13.9
Ours (Phi3.5-V [65])	4.2B	35.3	20.6	36.4	56.6	34.0
Ours (Qwen2-VL-2B [56])	2.2B	48.6	33.3	44.1	52.6	43.3
Ours (Qwen2-VL-7B [56])	8.3B	47.7	32.1	43.1	54.8	42.6

capabilities.

### B. Unlocking Zero-shot Power with Hierarchical Prompting

We first evaluate the ability of our prompt engineering to adapt a generative MLLM for discriminative tasks without any parameter updates.

1) *Zero-shot Performance on MMEB:* As demonstrated in Table II, our hierarchical prompt enables an off-the-shelf MLLM to achieve zero-shot performance comparable to models that have undergone extensive contrastive fine-tuning. This result validates our central hypothesis that an MLLM’s innate instruction-following capabilities can be systematically harnessed for discriminative tasks, presenting an efficient alternative to the dominant paradigm of resource-intensive pre-training. The framework’s effectiveness is particularly evident in the VQA and retrieval tasks, where the largest performance gains were observed.

2) *Zero-shot image-text compositionality:* To further probe the zero-shot capabilities of our prompt in fine-grained image-text alignment, we evaluate its performance on the SugarCrepes and SugarCrepes++ benchmarks. We compare our method against the VladVA baseline, which applies their representation prompt at the user-level prompt. As shown in the “Training-Free Prompting” section of Table VI, our hierarchical prompt enables the model to significantly surpass the VladVA baseline across all tested model sizes on both benchmarks, without any training. This superior zero-shot performance demonstrates our prompt’s effectiveness in unlocking nuanced embedding capacity from the MLLM, forcing a precise alignment between complex textual descriptions and visual components from the dataset.

3) *Analysis of Prompt Components:* To dissect the source of this strong zero-shot performance, we conducted two distinct ablation studies. First, to precisely measure the independent impact of each prompt component, we perform an ablation in a controlled setting that detaches the partially existing representation prompts from candidates in the MMEB benchmark. This analysis isolates the influence of applying a global system prompt and more granular representation

TABLE III: **Ablation study on prompt components in a controlled environment.** We measure the impact of applying the system prompt and representation prompts for the query (Rep<sub>Q</sub>) and candidate (Rep<sub>D</sub>). ‘w/ OW’ denotes the inclusion of the “in one word” keyword. This keyword is always applied to Rep<sub>Q</sub> since the query input already contains a task instruction. Avg. Task represents the average of the mean scores from all meta-tasks.

System	Rep <sub>Q</sub>	Rep <sub>D</sub>		Avg. Score	Avg. Task
		w/o OW	w/ OW		
X	X	X	X	13.94	15.26
	X	✓	X	24.21	24.47
	X	X	✓	33.74	34.34
	✓	X	✓	34.28	35.52
✓	X	X	X	42.29	42.99
	X	✓	X	<b>42.46</b>	43.30
	X	X	✓	41.44	42.23
	✓	X	X	<u>42.44</u>	<u>43.34</u>
	✓	✓	X	<b>42.46</b>	<b>43.49</b>
	✓	X	✓	41.71	42.72

TABLE IV: **Ablation on prompt strategies using the MMEB benchmark.** This study validates the effectiveness of different prompt combinations in a real-world setting.

Strategy	Cla.	VQA	Ret.	Gro.	Avg.
No-Prompt	21.0	8.7	9.1	26.1	14.2
System-Q	21.6	7.5	13.0	12.1	13.8
System-D	35.8	25.4	20.6	25.3	26.7
System-QD	46.7	31.8	<b>44.1</b>	46.7	41.7
+ QD-Rein.	45.8	30.3	37.1	46.7	39.1
+ D-Rein.	46.2	<b>33.3</b>	41.9	38.6	40.9
+ Q-Rein.	<b>48.6</b>	<b>33.3</b>	<b>44.1</b>	<b>52.6</b>	<b>43.3</b>

prompts (‘Rep’) that guide the model to produce a compressed output (e.g., using the keywords ‘in one word’). As shown in Table III, the results clearly demonstrate that the system prompt is the single most critical component; configurations that incorporate the system prompt consistently outperform those that omit it by a large margin. This experiment also indicates that adding a representation prompt for the query (Rep<sub>Q</sub>) on top of the system prompt leads to consistently strong performance, regardless of the presence or configuration of the candidate prompt (Rep<sub>D</sub>).

Moving from the controlled analysis, our second ablation study (Table IV) evaluates the template’s performance on the standard MMEB benchmark without any modifications. This tests the robustness of our approach against the natural variations and data noise present in the benchmark, unlike the previous experiment. We investigate various strategies for applying the system prompt. The optimal performance is achieved by applying the global system prompt to both queries and candidates, with a reinforcement cue applied only to the query (+ Q-Rein.). Conversely, applying the representation prompt to both query and candidate (+ QD-Rein.) degraded performance.

TABLE V: **Comparison with state-of-the-art methods on the MMEB benchmark.** Cla., VQA, Ret., Gro., IND, and OOD stand for Classification, VQA, Retrieval, Grounding, In-Domain, and Out-of-Domain, respectively. The highest score in each column is highlighted in bold. The second-best result is underlined.

Method	Model	#Params	Per Meta-Task Score				Average Score		
			Classification	VQA	Retrieval	Grounding	IND	OOD	Overall
#Datasets →			10	10	12	4	20	16	36
<i>Partially Supervised Finetuning Setting (Finetuning on M-BEIR)</i>									
GME [29]	Qwen2-VL	2.2B	56.9	41.2	67.8	53.4	-	-	55.8
MM-Embed [67]	LLaVA-1.6	7.8B	48.1	32.3	63.8	57.8	-	-	50.0
<i>Supervised Finetuning Setting (Finetuning on MMEB, &lt; 5B params)</i>									
OpenCLIP [61]	CLIP	0.4B	56.0	21.9	55.4	64.1	50.5	43.1	47.2
E5-V [17]	Phi3.5-V	4.2B	39.1	9.6	38.0	57.6	33.1	31.9	32.6
VLM2Vec [18]	Qwen2-VL	2.2B	59.0	49.4	65.4	73.4	66.0	52.6	59.3
VLM2Vec [18]	Phi-3.5-V	4.2B	54.8	54.9	62.3	79.5	66.5	52.0	60.1
UniME [28]	Phi-3.5-V	4.2B	54.8	55.9	64.5	81.8	68.2	52.7	64.2
CAFe [30]	LLaVA-OV [68]	0.9B	59.1	49.1	61.0	83.0	64.3	53.7	59.6
UNITE [32]	Qwen2-VL	2.2B	63.2	55.9	65.4	75.6	65.8	60.1	63.3
LLaVE [33]	Aquila-VL [69]	2.0B	62.1	<b>60.2</b>	65.2	<b>84.9</b>	69.4	59.8	65.2
Ours	Qwen2-VL	2.2B	<b>65.4</b>	59.1	<b>70.0</b>	83.0	<b>71.2</b>	<b>62.1</b>	<b>67.1</b>
<i>Supervised Finetuning Setting (Finetuning on MMEB, &gt; 5B params)</i>									
VLM2Vec [18]	LLaVA-1.6	7.6B	61.2	49.9	67.4	86.1	67.5	57.1	62.9
VLM2Vec [18]	Qwen2-VL	8.3B	62.6	57.8	69.9	81.7	72.2	57.8	65.8
MMRet [50]	LLaVA-1.6	7.6B	56.0	57.4	69.9	83.6	68.0	59.1	64.1
UniME [28]	LLaVA-1.6	7.6B	60.6	52.9	67.9	85.1	68.4	57.9	66.6
CAFe [30]	LLaVA-OV [68]	8.0B	65.2	65.6	70.0	91.2	75.8	62.4	69.8
UNITE [32]	Qwen2-VL	8.3B	68.3	65.1	71.6	84.8	73.6	66.3	70.3
LLaVE [33]	Aquila-VL [69]	8.0B	65.7	65.4	70.9	<b>91.9</b>	75.0	64.4	70.3
Ours	Qwen2-VL	8.3B	<b>69.1</b>	<b>67.3</b>	<b>74.1</b>	88.1	<b>76.4</b>	<b>67.4</b>	<b>72.4</b>

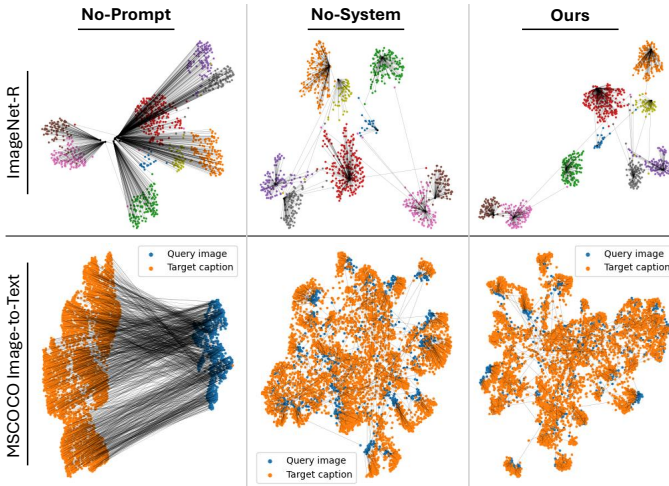


Fig. 4: **UMAP visualization of the zero-shot embedding space on ImageNet-R and MSCOCO Image-to-Text.**

### C. Qualitative Analysis of Embedding Space

To qualitatively assess the structure of the learned embedding space, we visualize the embeddings from the MMEB test set using Uniform Manifold Approximation and Projection (UMAP). As illustrated in Fig. 4, the base model without any prompt suffers from a severe modality gap, with image and text embeddings occupying separate spaces. Our hierarchical embedding prompt not only closes this gap decisively but also organizes the embeddings into remarkably compact and

semantically coherent clusters. This visualization provides qualitative proof that our systematic prompting is essential for guiding the MLLM to structure its capabilities into a discriminative and universal representation space.

### D. Efficient Hard negative training using SaHa

Building on our powerful zero-shot foundation, we fine-tune the model using our proposed self-aware hard negative sampling (SaHa) strategy to enhance the model’s discriminative capabilities.

1) *Fine-tuning Performance:* As shown in Table V, our framework demonstrates highly competitive results, outperforming other leading methods, including those reliant on large-scale contrastive pre-training. Specifically, our fine-tuned 2.2B model achieves a strong overall score of 67.1 and sets state-of-the-art performance in its parameter class for both the Classification (65.4) and Retrieval (70.0) tasks. This effectiveness scales with model size; our larger 8.3B model improves the overall score to 72.4 and also achieves state-of-the-art performance in the classification, VQA, and retrieval tasks. The framework’s exceptional performance in the Retrieval task, a known challenge for MLLMs, shows our framework’s effectiveness in mining challenging negatives to enhance the embeddings’ discriminative power.

2) *Fine-grained Compositionality Performance:* We assess our fine-tuned model’s performance on the SugarCrepes and SugarCrepes++ benchmarks. The results, detailed in the Contrastive Models sections of Table VI, are particularly note-



TABLE VI: Zero-shot results on SugarCrep and SugarCrep++ compositionality benchmark.

Method	Params	SugarCrep			SugarCrep++							
		Avg.	Swap Object		Swap Attribute		Replace Object		Replace Attribute		Replace Relation	
			ITT	TOT	ITT	TOT	ITT	TOT	ITT	TOT	ITT	TOT
Human	-	99.0	100.0	96.7	96.7	93.3	100.0	97.0	100.0	98.3	100.0	96.7
<i>Training-Free Prompting</i>												
VladVA (Qwen2-VL-2B)	2.21B	70.3	32.7	27.8	30.5	25.3	73.6	65.9	46.8	43.0	<u>57.6</u>	<b>58.3</b>
VladVA (LLaVA-1.5-7B)	7.06B	70.7	23.8	30.7	28.0	29.5	58.1	63.0	46.8	58.1	52.3	63.4
Ours (Qwen2-VL-2B)	2.21B	<u>76.6</u>	<u>41.2</u>	<u>31.0</u>	<u>36.8</u>	<u>30.2</u>	<b>84.0</b>	<u>81.4</u>	<b>61.5</b>	<b>63.8</b>	54.5	54.8
Ours (Qwen2-VL-7B)	8.21B	<b>77.6</b>	<b>44.1</b>	<b>35.9</b>	<b>40.8</b>	<b>38.7</b>	83.4	<b>85.7</b>	<u>59.5</u>	<u>60.0</u>	<b>58.8</b>	<u>58.1</u>
<i>Contrastive Models (&lt; 3B params)</i>												
OpenCLIP (ViT-G/14)	1.37B	80.1	40.7	27.4	54.2	49.6	93.1	89.4	72.5	73.1	57.6	51.4
OpenCLIP (ViT-BigG/14)	2.54B	82.0	48.8	28.2	57.7	<u>52.4</u>	94.2	90.5	<u>76.4</u>	72.6	59.4	53.6
VladVA (Qwen2-VL-2B)	2.21B	<b>88.2</b>	<b>50.8</b>	<u>33.5</u>	<b>60.4</b>	48.2	93.7	<u>93.8</u>	74.8	<u>77.5</u>	<u>63.6</u>	<u>57.4</u>
Ours (Qwen2-VL-2B)	2.21B	<u>87.0</u>	46.1	<b>38.4</b>	<u>59.5</u>	<b>55.4</b>	<b>95.6</b>	<b>81.9</b>	<b>85.5</b>	<b>72.0</b>	<b>64.4</b>	
<i>Contrastive Models (&gt; 3B params)</i>												
E5-V (LLaVA-1.5-7B)	7.06B	81.8	39.5	42.3	40.7	48.5	89.7	94.6	71.7	86.4	72.0	<u>81.5</u>
E5-V (LLaVA-Next-8B)	8.36B	84.2	50.8	48.4	49.7	56.9	93.1	<b>97.6</b>	76.1	<b>87.1</b>	<b>74.7</b>	<b>84.4</b>
VLM2Vec (LLaVA-1.6-7B)	7.30B	83.8	40.7	39.9	48.1	50.0	94.6	96.9	77.0	85.6	67.9	70.7
VladVA (LLaVA-1.5-7B)	7.06B	<b>90.0</b>	<b>56.1</b>	36.7	<u>63.0</u>	<u>62.5</u>	<b>95.0</b>	93.0	<u>78.2</u>	82.3	71.1	66.3
Ours (Qwen2-VL-7B)	8.21B	<u>87.5</u>	<u>51.0</u>	<b>51.0</b>	<b>73.1</b>	<b>77.8</b>	94.2	93.4	<b>82.2</b>	83.1	<u>73.1</u>	71.8

TABLE VII: Performance comparison of various negative sampling strategies. The training time is based on 1.5 epochs.

Prompt	Sampling	Hyperparams		Training Time (hr)	Performance		
		# HN	# Batch		IND	OOD	Avg.
-	In-batch	-	1024	-	66.0	52.6	59.3
Ours	In-batch	-	1024	13.7	68.5	58.6	64.1
	HN	1	256	20.7	60.8	51.4	56.6
		7	256	59.7	62.6	54.0	58.8
	HN + $\beta$ [28]	7	256	59.7	67.2	58.1	63.1
	Saha (Ours)	7	256	15.8	70.8	62.0	66.9
		15	128	16.1	<b>71.2</b>	<b>62.1</b>	<b>67.1</b>

worthy when considering the training data disparity. Our model was fine-tuned on approximately 0.8M multi-task pairs, whereas a strong baseline like VladVA utilized 8.1M image-caption pairs in a large-scale contrastive learning setup—a regimen more directly aligned with SugarCrep’s image-caption retrieval format.

Despite this significant disadvantage in both data volume and task alignment, our approach achieves highly competitive, and in several key categories, superior performance. On SugarCrep++, for instance, our 7B model demonstrates remarkable strength in the ‘Swap Attribute’ category, outperforming the baseline significantly. The ability to attain such strong compositional understanding with only a fraction ( $\sim 10\%$ ) of the domain-specific training data highlights the fundamental efficiency and effectiveness of our framework.

3) *Analysis of Sampling Strategies:* To validate the effectiveness of SaHa, we compare it against several baselines. (1) In-batch Negative Sampling: A standard contrastive learning strategy where other positive samples within the same mini-batch are used as negatives. (2) Hard Negative (HN) Sampling: We implement a classical online hard negative mining strategy. For each anchor within a training batch, we use the model’s current encoder to perform a global search across the entire

TABLE VIII: Sensitivity analysis for the pool multiplier in SaHa ( $k = 7$ ). The pool multiplier denotes the size of the initial candidate pool relative to the number of negatives ( $k$ )

Metric	Baseline	Pool Multiplier		
		4	6	8
IND	62.6	<b>70.8</b>	70.7	70.6
OND	54.0	<b>62.0</b>	61.9	61.6
Avg.	58.8	<b>66.9</b>	66.8	66.6

candidate corpus and select the top-k most semantically similar documents as hard negatives. (3) HN +  $\beta$  [28]: We re-implement the false negative mitigation strategy, which filters out hard negatives whose similarity score to the query exceeds a certain threshold. Following an empirical analysis based on the standard deviation of embedding similarities on retrieval tasks, the threshold  $\beta$  was set to 0.02 in our experiments.

In Table VII, our analysis reveals a key limitation of conventional hard negative (HN) mining: fine-tuning with in-batch negatives substantially outperforms HN-based fine-tuning, because HN mining frequently treats unlabeled positives as negatives (i.e., introduces false negatives), which degrades learning.

This finding highlights two important aspects of our framework. First, the hierarchical prompt constructs a high-quality initial embedding space, so well-structured that even simple in-batch sampling yields strong performance. Second, the superior results from in-batch sampling motivate a more principled and context-aware alternative to conventional HN mining. SaHa is designed to be this alternative, addressing the false negative issue while achieving better scores with only a fraction of the training time. Collectively, these observations demonstrate that SaHa is not merely a faster variant, but a more robust and effective training strategy.

Furthermore, to show the robustness of our strategy, we

conduct a sensitivity analysis on its key hyperparameter, the pool multiplier, with the results shown in Table VIII. The pool multiplier controls the ratio between the initial candidate pool size and the final number of selected hard negatives ( $k$ ). For example, with  $k=7$  and a pool multiplier of 4, our method first constructs a candidate query pool of 28 before selecting the 7 most effective hard negatives. As presented in the table, all tested multiplier settings achieve substantial gains over the baseline. We observe a slight and graceful degradation in performance as the multiplier increases from 4 to 8; nevertheless, the performance remains remarkably stable, with only marginal differences across the tested values. This low sensitivity demonstrates the robustness of our SaHa strategy, indicating that it does not require meticulous hyperparameter tuning to deliver high performance, further highlighting its practical advantages.

## V. CONCLUSION

In this paper, we mitigate the inefficient adaptation of MLLMs for universal multimodal embedding tasks. To elicit the zero-shot discriminative ability of MLLMs, we diverge from prior works that focused on text transformation. We instead concentrate on systematically structuring prompts to generate embeddings. We observed that system prompts yield higher attention efficiency than user prompts. Based on this, we design a hierarchical embedding prompt template with two levels of instructions (system-level and user-level) to construct a discriminative representation space. We demonstrate that this prompting strategy alone achieves performance competitive with MLLM baselines that have undergone extensive contrastive pre-training. We also validate this result through rigorous ablation studies. Building on the strong discriminative capabilities endowed by our prompt, we introduce Self-aware Hard Negative Sampling (SaHa), a hard-negative sampling strategy guided by the model’s own understanding. For each anchor query, SaHa identifies challenging negatives that remain semantically distinct, grouping them to prevent false negative contamination. This approach also enhances training efficiency by minimizing the redundant inferences common in traditional hard negative sampling methods. After fine-tuning on the MMEB dataset using a training set pre-processed by SaHa, our model achieves state-of-the-art performance, outperforming baselines including those reliant on large-scale contrastive pre-training. For future work, we plan to extend our framework to additional modalities such as video and audio. We will also investigate methods to preserve the model’s generative capabilities alongside its discriminative performance, particularly under limited computational resources.

## REFERENCES

- [1] T. Mikolov, I. Sutskever, K. Chen, G. S. Corrado, and J. Dean, “Distributed representations of words and phrases and their compositionality,” *Advances in neural information processing systems (NeurIPS)*, vol. 26, 2013.
- [2] J. Devlin, M.-W. Chang, K. Lee, and K. Toutanova, “BERT: Pre-training of deep bidirectional transformers for language understanding,” in *Proceedings of the conference of the North American chapter of the association for computational linguistics (NAACL)*, 2019, pp. 4171–4186.
- [3] T. Wang, X. Zhang, L. Lan, and Z. Luo, “Local-to-global deep clustering on approximate uniform manifold,” *IEEE Transactions on Knowledge and Data Engineering (TKDE)*, vol. 35, no. 5, pp. 5035–5046, 2023.
- [4] Y. Yang, D.-C. Zhan, Y.-F. Wu, Z.-B. Liu, H. Xiong, and Y. Jiang, “Semi-supervised multi-modal clustering and classification with incomplete modalities,” *IEEE Transactions on Knowledge and Data Engineering (TKDE)*, vol. 33, no. 2, pp. 682–695, 2019.
- [5] V. Karpukhin, B. Oguz, S. Min, P. Lewis, L. Wu, S. Edunov, D. Chen, and W.-t. Yih, “Dense passage retrieval for open-domain question answering,” in *Proceedings of the 2020 Conference on Empirical Methods in Natural Language Processing (EMNLP)*, B. Webber, T. Cohn, Y. He, and Y. Liu, Eds., 2020, pp. 6769–6781.
- [6] H. Tan, S. Zhan, H. Lin, H.-T. Zheng, and W. K. Chan, “QAEA-DR: A unified text augmentation framework for dense retrieval,” *IEEE Transactions on Knowledge and Data Engineering (TKDE)*, vol. 37, no. 6, pp. 3669–3683, 2025.
- [7] N. Passalis and A. Tefas, “Entropy optimized feature-based bag-of-words representation for information retrieval,” *IEEE Transactions on Knowledge and Data Engineering (TKDE)*, vol. 28, no. 7, pp. 1664–1677, 2016.
- [8] P. Lewis, E. Perez, A. Piktus, F. Petroni, V. Karpukhin, N. Goyal, H. Küttler, M. Lewis, W.-t. Yih, T. Rocktäschel *et al.*, “Retrieval-augmented generation for knowledge-intensive nlp tasks,” *Advances in neural information processing systems (NeurIPS)*, vol. 33, pp. 9459–9474, 2020.
- [9] N. Muennighoff, N. Tazi, L. Magne, and N. Reimers, “MTEB: Massive text embedding benchmark,” in *Proceedings of the Conference of the European Chapter of the Association for Computational Linguistics (EACL)*, 2023, pp. 2014–2037.
- [10] H. Su, W. Shi, J. Kasai, Y. Wang, Y. Hu, M. Ostendorf, W.-t. Yih, N. A. Smith, L. Zettlemoyer, and T. Yu, “One embedder, any task: Instruction-finetuned text embeddings,” in *Findings of the Association for Computational Linguistics (ACL)*, 2023, pp. 1102–1121.
- [11] A. Asai, T. Schick, P. Lewis, X. Chen, G. Izacard, S. Riedel, H. Hajishirzi, and W.-t. Yih, “Task-aware retrieval with instructions,” in *Findings of the Association for Computational Linguistics (ACL)*, 2023, pp. 3650–3675.
- [12] J. Ni, C. Qu, J. Lu, Z. Dai, G. Hernandez Abrego, J. Ma, V. Zhao, Y. Luan, K. Hall, M.-W. Chang, and Y. Yang, “Large dual encoders are generalizable retrievers,” in *Proceedings of the Conference on Empirical Methods in Natural Language Processing (EMNLP)*, 2022, pp. 9844–9855.
- [13] L. Wang, N. Yang, X. Huang, B. Jiao, L. Yang, D. Jiang, R. Majumder, and F. Wei, “Text embeddings by weakly-supervised contrastive pre-training,” *arXiv preprint arXiv:2212.03533*, 2022.
- [14] J. Chen, S. Xiao, P. Zhang, K. Luo, D. Lian, and Z. Liu, “BGE M3-embedding: Multi-lingual, multi-functionality, multi-granularity text embeddings through self-knowledge distillation,” *arXiv preprint arXiv:2402.03216*, 2024.
- [15] Z. Liu, C. Xiong, Y. Lv, Z. Liu, and G. Yu, “Universal vision-language dense retrieval: Learning a unified representation space for multi-modal retrieval,” in *The International Conference on Learning Representations (ICLR)*, 2023.
- [16] J. Zhou, Z. Liu, S. Xiao, B. Zhao, and Y. Xiong, “VISTA: Visualized text embedding for universal multi-modal retrieval,” in *Proceedings of the Annual Meeting of the Association for Computational Linguistics (ACL)*, 2024, pp. 3185–3200.
- [17] T. Jiang, M. Song, Z. Zhang, H. Huang, W. Deng, F. Sun, Q. Zhang, D. Wang, and F. Zhuang, “E5-V: Universal embeddings with multimodal large language models,” *arXiv preprint arXiv:2407.12580*, 2024.
- [18] Z. Jiang, R. Meng, X. Yang, S. Yavuz, Y. Zhou, and W. Chen, “VLM2vec: Training vision-language models for massive multimodal embedding tasks,” in *The International Conference on Learning Representations (ICLR)*, 2025.
- [19] A. Baldrati, M. Bertini, T. Uricchio, and A. Del Bimbo, “Composed image retrieval using contrastive learning and task-oriented clip-based features,” *ACM Transactions on Multimedia Computing, Communications and Applications (TOMM)*, vol. 20, no. 3, pp. 1–24, 2023.
- [20] C. Wei, Y. Chen, H. Chen, H. Hu, G. Zhang, J. Fu, A. Ritter, and W. Chen, “Uniir: Training and benchmarking universal multimodal information retrievers,” in *European Conference on Computer Vision (ECCV)*, 2024, pp. 387–404.
- [21] A. Radford, J. W. Kim, C. Hallacy, A. Ramesh, G. Goh, S. Agarwal, G. Sastry, A. Askell, P. Mishkin, J. Clark *et al.*, “Learning transferable visual models from natural language supervision,” in *International Conference on Machine Learning (ICML)*, 2021, pp. 8748–8763.

- [22] J. Li, D. Li, C. Xiong, and S. Hoi, “BLIP: Bootstrapping language-image pre-training for unified vision-language understanding and generation,” in *International Conference on Machine Learning (ICML)*, 2022, pp. 12 888–12 900.
- [23] W. Lin, J. Chen, J. Mei, A. Coca, and B. Byrne, “Fine-grained late-interaction multi-modal retrieval for retrieval augmented visual question answering,” *Advances in Neural Information Processing Systems (NeurIPS)*, vol. 36, 2023.
- [24] M. Luo, Z. Fang, T. Gokhale, Y. Yang, and C. Baral, “End-to-end knowledge retrieval with multi-modal queries,” in *Proceedings of the Annual Meeting of the Association for Computational Linguistics (ACL)*, 2023, pp. 8573–8589.
- [25] Y.-J. Ju, H.-J. Kim, and S.-W. Lee, “MIRe: Enhancing multimodal queries representation via fusion-free modality interaction for multi-modal retrieval,” in *Findings of the Annual Meeting of the Association for Computational Linguistics (ACL)*, 2025, pp. 5350–5363.
- [26] S. Song, X. Li, S. Li, S. Zhao, J. Yu, J. Ma, X. Mao, W. Zhang, and M. Wang, “How to bridge the gap between modalities: Survey on multimodal large language model,” *IEEE Transactions on Knowledge and Data Engineering (TKDE)*, 2025.
- [27] J. Wei, Y. Tay, R. Bommasani, C. Raffel, B. Zoph, S. Borgeaud, D. Yogatama, M. Bosma, D. Zhou, D. Metzler, E. H. Chi, T. Hashimoto, O. Vinyals, P. Liang, J. Dean, and W. Fedus, “Emergent abilities of large language models,” *Transactions on Machine Learning Research (TMLR)*, 2022.
- [28] T. Gu, K. Yang, Z. Feng, X. Wang, Y. Zhang, D. Long, Y. Chen, W. Cai, and J. Deng, “Breaking the modality barrier: Universal embedding learning with multimodal llms,” *arXiv preprint arXiv:2504.17432*, 2025.
- [29] X. Zhang, Y. Zhang, W. Xie, M. Li, Z. Dai, D. Long, P. Xie, M. Zhang, W. Li, and M. Zhang, “Bridging modalities: Improving universal multimodal retrieval by multimodal large language models,” in *Proceedings of the Computer Vision and Pattern Recognition Conference (CVPR)*, 2025, pp. 9274–9285.
- [30] H. Yu, Z. Zhao, S. Yan, L. Korycki, J. Wang, B. He, J. Liu, L. Zhang, X. Fan, and H. Yu, “CAFe: Unifying representation and generation with contrastive-autoregressive finetuning,” *arXiv preprint arXiv:2503.19900*, 2025.
- [31] Y. Ouali, A. Bulat, A. Xenos, A. Zaganidis, I. M. Metaxas, B. Martinez, and G. Tzimiropoulos, “VladVA: Discriminative fine-tuning of lylms,” in *Proceedings of the Computer Vision and Pattern Recognition (CVPR)*, 2025, pp. 4101–4111.
- [32] F. Kong, J. Zhang, Y. Liu, H. Zhang, S. Feng, X. Yang, D. Wang, Y. Tian, F. Zhang, G. Zhou *et al.*, “Modality curation: Building universal embeddings for advanced multimodal information retrieval,” *arXiv preprint arXiv:2505.19650*, 2025.
- [33] Z. Lan, L. Niu, F. Meng, J. Zhou, and J. Su, “Llave: Large language and vision embedding models with hardness-weighted contrastive learning,” *arXiv preprint arXiv:2503.04812*, 2025.
- [34] S. Robertson, H. Zaragoza *et al.*, “The probabilistic relevance framework: Bm25 and beyond,” *Foundations and Trends® in Information Retrieval*, pp. 333–389, 2009.
- [35] K. Lee, M.-W. Chang, and K. Toutanova, “Latent retrieval for weakly supervised open domain question answering,” in *Proceedings of the Annual Meeting of the Association for Computational Linguistics (ACL)*, 2019, pp. 6086–6096.
- [36] G. Izacard, M. Caron, L. Hosseini, S. Riedel, P. Bojanowski, A. Joulin, and E. Grave, “Unsupervised dense information retrieval with contrastive learning,” *Transactions on Machine Learning Research (TMLR)*, 2022.
- [37] J. Chen, S. Xiao, P. Zhang, K. Luo, D. Lian, and Z. Liu, “M3-embedding: Multi-linguality, multi-functionality, multi-granularity text embeddings through self-knowledge distillation,” in *Findings of the Association for Computational Linguistics (ACL)*, 2024, pp. 2318–2335.
- [38] C. Raffel, N. Shazeer, A. Roberts, K. Lee, S. Narang, M. Matena, Y. Zhou, W. Li, and P. J. Liu, “Exploring the limits of transfer learning with a unified text-to-text transformer,” *The Journal of Machine Learning Research (JMLR)*, vol. 21, no. 1, 2020.
- [39] C. Qu, H. Zamani, L. Yang, W. B. Croft, and E. Learned-Miller, “Passage retrieval for outside-knowledge visual question answering,” in *Proceedings of the International ACM SIGIR Conference on Research and Development in Information Retrieval (SIGIR)*, 2021, pp. 1753–1757.
- [40] F. Gao, Q. Ping, G. Thattai, A. Reganti, Y. N. Wu, and P. Natarajan, “A thousand words are worth more than a picture: Natural language-centric outside-knowledge visual question answering,” *arXiv preprint arXiv:2201.05299*, 2022.
- [41] A. Salemi, J. Altmayer Pizzorno, and H. Zamani, “A symmetric dual encoding dense retrieval framework for knowledge-intensive visual question answering,” in *Proceedings of the International ACM SIGIR Conference on Research and Development in Information Retrieval (SIGIR)*, 2023, pp. 110–120.
- [42] L. Gui, B. Wang, Q. Huang, A. Hauptmann, Y. Bisk, and J. Gao, “KAT: A knowledge augmented transformer for vision-and-language,” in *Proceedings of the Conference of the North American Chapter of the Association for Computational Linguistics (NAACL)*, 2022, pp. 956–968.
- [43] Z. Yang, Z. Gan, J. Wang, X. Hu, Y. Lu, Z. Liu, and L. Wang, “An empirical study of gpt-3 for few-shot knowledge-based vqa,” in *Proceedings of the Association for the Advancement of Artificial Intelligence (AAAI)*, vol. 36, no. 3, 2022, pp. 3081–3089.
- [44] J. Wu and R. Mooney, “Entity-focused dense passage retrieval for outside-knowledge visual question answering,” in *Proceedings of the Conference on Empirical Methods in Natural Language Processing (EMNLP)*, 2022, pp. 8061–8072.
- [45] X. Ma, L. Wang, N. Yang, F. Wei, and J. Lin, “Fine-tuning llama for multi-stage text retrieval,” in *Proceedings of the International ACM SIGIR Conference on Research and Development in Information Retrieval (SIGIR)*, 2024, pp. 2421–2425.
- [46] C. Li, Z. Liu, S. Xiao, Y. Shao, and D. Lian, “Llama2vec: Unsupervised adaptation of large language models for dense retrieval,” in *Proceedings of the Annual Meeting of the Association for Computational Linguistics (ACL)*, 2024, pp. 3490–3500.
- [47] C. Li, M. Qin, S. Xiao, J. Chen, K. Luo, D. Lian, Y. Shao, and Z. Liu, “Making text embedders few-shot learners,” in *The International Conference on Learning Representations (ICLR)*, 2025.
- [48] C. Lee, R. Roy, M. Xu, J. Raiman, M. Shoenybi, B. Catanzaro, and W. Ping, “NV-embed: Improved techniques for training LLMs as generalist embedding models,” in *The International Conference on Learning Representations (ICLR)*, 2025.
- [49] S.-C. Lin, C. Lee, M. Shoenybi, J. Lin, B. Catanzaro, and W. Ping, “MM-EMBED: Universal multimodal retrieval with multimodal llms,” in *The International Conference on Learning Representations (ICLR)*, 2025.
- [50] J. Zhou, Z. Liu, Z. Liu, S. Xiao, Y. Wang, B. Zhao, C. J. Zhang, D. Lian, and Y. Xiong, “Megapairs: Massive data synthesis for universal multimodal retrieval,” *arXiv preprint arXiv:2412.14475*, 2024.
- [51] A. Dosovitskiy, L. Beyer, A. Kolesnikov, D. Weissenborn, X. Zhai, T. Unterthiner, M. Dehghani, M. Minderer, G. Heigold, S. Gelly, J. Uszkoreit, and N. Houlsby, “An image is worth 16x16 words: Transformers for image recognition at scale,” in *International Conference on Learning Representations (ICLR)*, 2021.
- [52] H. Touvron, T. Lavril, G. Izacard, X. Martinet, M.-A. Lachaux, T. Lacroix, B. Rozière, N. Goyal, E. Hambro, F. Azhar *et al.*, “LLaMA: Open and efficient foundation language models,” *arXiv preprint arXiv:2302.13971*, 2023.
- [53] L. Chen, H. Zhao, T. Liu, S. Bai, J. Lin, C. Zhou, and B. Chang, “An image is worth 1/2 tokens after layer 2: Plug-and-play inference acceleration for large vision-language models,” in *European Conference on Computer Vision (ECCV)*. Springer, 2024, pp. 19–35.
- [54] S. Zhang, Q. Fang, Z. Yang, and Y. Feng, “LLaVA-mini: Efficient image and video large multimodal models with one vision token,” in *The International Conference on Learning Representations (ICLR)*, 2025.
- [55] A. v. d. Oord, Y. Li, and O. Vinyals, “Representation learning with contrastive predictive coding,” *arXiv preprint arXiv:1807.03748*, 2018.
- [56] P. Wang, S. Bai, S. Tan, S. Wang, Z. Fan, J. Bai, K. Chen, X. Liu, J. Wang, W. Ge *et al.*, “Qwen2-VL: Enhancing vision-language model’s perception of the world at any resolution,” *arXiv preprint arXiv:2409.12191*, 2024.
- [57] I. Loshchilov and F. Hutter, “Decoupled weight decay regularization,” in *International Conference on Learning Representations (ICLR)*, 2019.
- [58] L. Gao, Y. Zhang, J. Han, and J. Callan, “Scaling deep contrastive learning batch size under memory limited setup,” in *Proceedings of the Workshop on Representation Learning for NLP (RepLanLP)*, A. Rogers, I. Calixto, I. Vulić, N. Saphra, N. Kassner, O.-M. Camburu, T. Bansal, and V. Shwartz, Eds., 2021, pp. 316–321.
- [59] C.-Y. Hsieh, J. Zhang, Z. Ma, A. Kembhavi, and R. Krishna, “Sugarcrepe: Fixing hackable benchmarks for vision-language compositionality,” *Advances in Neural Information Processing Systems (NeurIPS)*, vol. 36, pp. 31 096–31 116, 2023.
- [60] S. H. Dumpala, A. Jaiswal, C. S. Sastry, E. Milios, S. Oore, and H. Sajjad, “SUGARCREPE++ dataset: Vision-language model sensitivity to semantic and lexical alterations,” in *The Conference on Neural Information Processing Systems (NeurIPS): Datasets and Benchmarks Track*, 2024.
- [61] M. Cherti, R. Beaumont, R. Wightman, M. Wortsman, G. Ilharco, C. Gordon, C. Schuhmann, L. Schmidt, and J. Jitsev, “Reproducible scaling laws for contrastive language-image learning,” in *Proceedings of*

- the *IEEE/CVF Conference on Computer Vision and Pattern Recognition (CVPR)*, 2023, pp. 2818–2829.
- [62] X. Zhai, B. Mustafa, A. Kolesnikov, and L. Beyer, “Sigmoid loss for language image pre-training,” in *Proceedings of the IEEE/CVF International Conference on Computer Vision (ICCV)*, 2023, pp. 11 975–11 986.
  - [63] K. Zhang, Y. Luan, H. Hu, K. Lee, S. Qiao, W. Chen, Y. Su, and M.-W. Chang, “MagicLens: self-supervised image retrieval with open-ended instructions,” in *Proceedings of the International Conference on Machine Learning (ICML)*, 2024.
  - [64] F. Li, R. Zhang, H. Zhang, Y. Zhang, B. Li, W. Li, Z. MA, and C. Li, “LLaVA-neXT-interleave: Tackling multi-image, video, and 3d in large multimodal models,” in *The International Conference on Learning Representations (ICLR)*, 2025.
  - [65] M. Abdin, J. Aneja, H. Awadalla, A. Awadallah, A. A. Awan, N. Bach, A. Bahree, A. Bakhtiari, J. Bao, H. Behl *et al.*, “Phi-3 technical report: A highly capable language model locally on your phone,” *arXiv preprint arXiv:2404.14219*, 2024.
  - [66] H. Liu, C. Li, Y. Li, and Y. J. Lee, “Improved baselines with visual instruction tuning,” in *Proceedings of the IEEE/CVF Conference on Computer Vision and Pattern Recognition (CVPR)*, 2024, pp. 26 296–26 306.
  - [67] S.-C. Lin, C. Lee, M. Shoenybi, J. Lin, B. Catanzaro, and W. Ping, “MM-Embed: Universal multimodal retrieval with multimodal llms,” in *The International Conference on Learning Representations (ICLR)*, 2025.
  - [68] B. Li, Y. Zhang, D. Guo, R. Zhang, F. Li, H. Zhang, K. Zhang, P. Zhang, Y. Li, Z. Liu, and C. Li, “LLaVA-onevision: Easy visual task transfer,” *Transactions on Machine Learning Research (TMLR)*, 2025.
  - [69] S. Gu, J. Zhang, S. Zhou, K. Yu, Z. Xing, L. Wang, Z. Cao, J. Jia, Z. Zhang, Y. Wang *et al.*, “Infinity-mm: Scaling multimodal performance with large-scale and high-quality instruction data,” *arXiv preprint arXiv:2410.18558*, 2024.